



Cite this: *Phys. Chem. Chem. Phys.*,
2021, **23**, 5927

Decrease in sulfate aerosol light backscattering by reactive uptake of isoprene epoxydiols†

C. Dubois,^a D. Cholleton,^b R. Gemayel,^a Y. Chen,^c J. D. Surratt,^{cd}
C. George,^a P. Rairoux,^b A. Miffre^{ab} and M. Riva^{ab*}

Sulfate aerosol is responsible for a net cooling of the Earth's atmosphere due to its ability to backscatter light. Through atmospheric multiphase chemistry, it reacts with isoprene epoxydiols leading to the formation of aerosol and organic compounds, including organosulfates and high-molecular weight compounds. In this study, we evaluate how sulfate aerosol light backscattering is modified in the presence of such organic compounds. Our laboratory experiments show that reactive uptake of isoprene epoxydiols on sulfate aerosol is responsible for a decrease in light backscattering compared to pure inorganic sulfate particles of up to – 12% at 355 nm wavelength and – 21% at 532 nm wavelength. Moreover, while such chemistry is known to yield a core-shell structure, the observed reduction in the backscattered light intensity is discussed with Mie core-shell light backscattering numerical simulations. We showed that the observed decrease can only be explained by considering effects from the complex optical refractive index. Since isoprene is the most abundant hydrocarbon emitted into the atmosphere, and isoprene epoxydiols are the most important isoprene secondary organic aerosol precursors, our laboratory findings can aid in quantifying the direct radiative forcing of sulfates in the presence of organic compounds, thus more clearly resolving the impact of such aerosol particles on the Earth's climate.

Received 19th October 2020,
Accepted 18th February 2021

DOI: 10.1039/d0cp05468b

rsc.li/pccp

Introduction

Atmospheric aerosols directly contribute to the Earth's radiative balance through light scattering and absorption.¹ Hence, sulfate aerosols produce a net negative radiative forcing^{2–5} that is attributed to their ability to backscatter solar radiation.⁶ Conversely, the impact of organic aerosol on the Earth's radiative balance remains elusive as it is associated with large uncertainties.^{6–10} While it was assumed that sulfur is primarily present in its inorganic forms (e.g., SO_4^{2-} , HSO_4^- , HSO_3^-), field and laboratory studies^{11–15} recently showed that organosulfur compounds, including organosulfates, are important contributors to the total sulfate aerosol mass. For example, Surratt *et al.*¹⁵ have reported that organosulfates can contribute to a substantial fraction of the organic aerosol mass

(i.e., up to 30%). Among the chemical processes leading to organosulfates, recent studies have highlighted the importance of multiphase chemistry (reactive uptake) of isoprene epoxydiols (IEPOX).^{16–22} Hence, IEPOX have been shown to be key products formed from the hydroxyl radical (OH)-initiated oxidation of isoprene,²³ which is the most abundant non-methane volatile organic compound emitted into the atmosphere.²⁴ Once produced, gaseous IEPOX can undergo acid-driven multiphase chemistry yielding a wide variety of oxygenated compounds including C_5 alkene triols,²⁵ 2-methyltetrols,^{26,27} hemiacetal dimers,²⁸ *cis*- and *trans*-3-methyltetra hydrofuran-3,4-diols,¹⁷ and organosulfates (e.g., IEPOX-OSS),^{11,29–31} contributing to the formation of secondary organic aerosols (SOA). Moreover, the reactive uptake of IEPOX on sulfate aerosol leads to a substantial inorganic-to-organic sulfate conversion (i.e., up to 90%) and increases as a function of IEPOX-to-inorganic sulfate ratio.¹¹ For example, organosulfates have been estimated to account for 16.5% of the total organic carbon found in fine particulate matter $\text{PM}_{2.5}$ collected from downtown Atlanta, GA.³² IEPOX-OSS (e.g., 2-methyltetrol sulfate isomers) represented in this study, 12.6% of these organosulfates. As an important result, in the presence of acidic sulfate aerosol, IEPOX modifies the aerosol chemical composition, as revealed in recent studies.^{11,21,22,33} For example, a net modification of the aerosol morphology from a well-mixed sphere to a core-shell structure has been

^a Univ. Lyon, Université Claude Bernard Lyon 1, CNRS, IRCELYON,
F-69626, Villeurbanne, France. E-mail: matthieu.riva@ircelyon.univ-lyon1.fr

^b Univ. Lyon, Université Claude Bernard Lyon 1, CNRS, Institut Lumière Matière,
F-69622, Villeurbanne, France. E-mail: alain.miffre@univ-lyon1.fr

^c Department of Environmental Sciences and Engineering, Gillings School of Global
Public Health, The University of North Carolina at Chapel Hill, Chapel Hill, NC,
USA

^d Department of Chemistry, The University of North Carolina at Chapel Hill,
Chapel Hill, NC, USA

† Electronic supplementary information (ESI) available. See DOI: 10.1039/d0cp05468b

reported,^{11,21,22} which is anticipated to impact the aerosol physicochemical properties.¹¹

Light backscattering is a physical process sensitive to the aerosol number concentration, size, shape and chemical composition through the particles complex refractive index.^{34–37} Very recently, Reid *et al.* interestingly showed that light scattering can be used to detect the aerosol morphology of individual particles.³⁸ By light backscattering, we here intend light scattering in the exact (*i.e.*, strict) backward scattering direction of π or 180.0° , hence far from the 90° to 170° scattering angles, often reported in the literature as backward scattering direction. Light scattering may indeed vary when the scattering angle differs from the exact π backscattering angle, as we demonstrated.³⁹ Moreover, precise knowledge of the backward scattering direction of π is required for accurate radiative transfer calculations.⁴⁰ Until recently, measuring exact light backscattering by particles embedded in laboratory ambient air represented an experimental challenge, mainly due to the finite size of the detector and the need for a high angular resolution, to specifically address the backward scattering direction with high accuracy ($180.0^\circ \pm 0.2^\circ$). These difficulties have been recently overcome⁴¹ and it is now possible to conduct laboratory experiments in order to accurately quantify the light backscattered by aerosols.

In this paper, controlled-laboratory experiments were performed to quantify the modification of light backscattering due to the reactive uptake of gaseous IEPOX on acidic sulfate aerosol particles. Hence, acidified ammonium sulfate (AAS) seed aerosols were generated and chemically characterized in the presence and in the absence of IEPOX. To confirm the formation of IEPOX-SOA, the resulting organic products, *i.e.*, organosulfates, were quantified using an ultra-high performance liquid chromatography methodology, interfaced with an electrospray ionization-mass spectrometer (UHPLC/ESI-MS). In the meantime, the ability of IEPOX-SOA to backscatter light was quantified in the exact (*i.e.*, strict) backward scattering direction of π , by using a unique optical experimental setup, issued from recent advances in laboratory light scattering by atmospheric aerosols, as stated above.⁴¹ We then compare our laboratory findings with the outputs given by Lorenz-Mie light scattering numerical simulations.

Our results interestingly reveal that reactive uptake of IEPOX on acidified sulfate particles reduces light backscattering compared to pure inorganic sulfates. This finding suggests that, when organic compounds, including organosulfates and high-molecular weight compounds, are present, the ability of inorganic sulfate particles to backscatter light is greatly decreased.

Experimental section

Material and instruments

Aerosol generation and characterization. Fig. 1 presents the flow tube experiment used to generate the IEPOX-SOA and AAS aerosols. The methodology used for the generation of sulfate aerosols and IEPOX was similar to the one previously used,^{42,43} and this chemistry has been shown to produce aerosols with core-shell structures.^{11,21,22} Due to the lack of IEPOX-SOA standards, it was not possible to generate well-mixed aerosols containing IEPOX-derived SOA components. The aerosol seed particles were generated with a constant output atomizer containing AAS. Gas-phase IEPOX was generated after bubbling high-purity nitrogen into a solution of *trans*- β -IEPOX diluted into ethyl acetate; *trans*- β -IEPOX was synthesized in-house as described earlier.⁴⁴ Both were sent through a 6 L large aerosol flow tube reactor. Aerosol particle number, size and volume were determined using a differential mobility analyzer (DMA, TSI Inc., model 3080) coupled with an ultrafine condensation particle counter (CPC, TSI Inc., model 3776). As the particle size modifies the backscattered light intensity, the absence of larger particles (*i.e.*, with diameter $>1\ \mu\text{m}$) was monitored using an optical particle sizer (OPS, TSI Inc., model 3330). During the IEPOX uptake experiments onto the AAS seed aerosol, the AAS seed aerosols produced from the atomizer were size-selected by a DMA at the entrance of the aerosol flow tube to be centered at $145 \pm 40\ \text{nm}$ (Fig. S1, ESI†).

A synthetic air flow (Air Products, 80/20) of $6\ \text{L min}^{-1}$ was used, corresponding to a residence time of 1 minute in the flow tube reactor. The relative humidity (RH) was held constant at $\sim 49 \pm 3\%$ during all the experiments (Fig. S2, ESI†), corresponding to

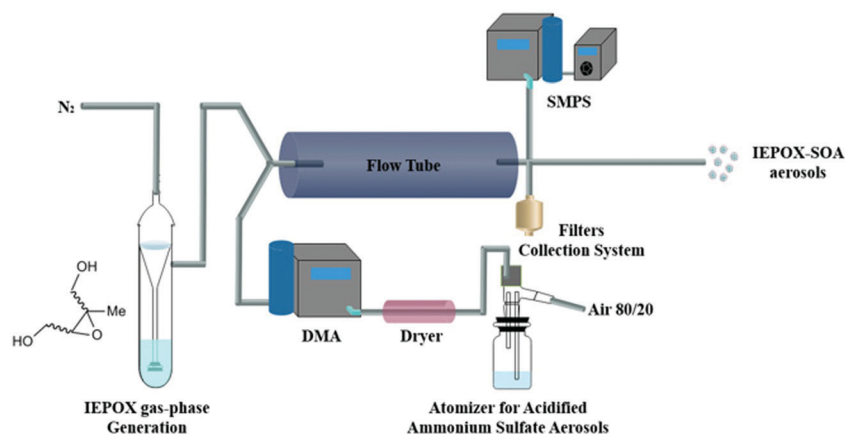


Fig. 1 Schematic of our laboratory experimental set-up for generating IEPOX-SOA, which is similar to prior studies.^{42,43}

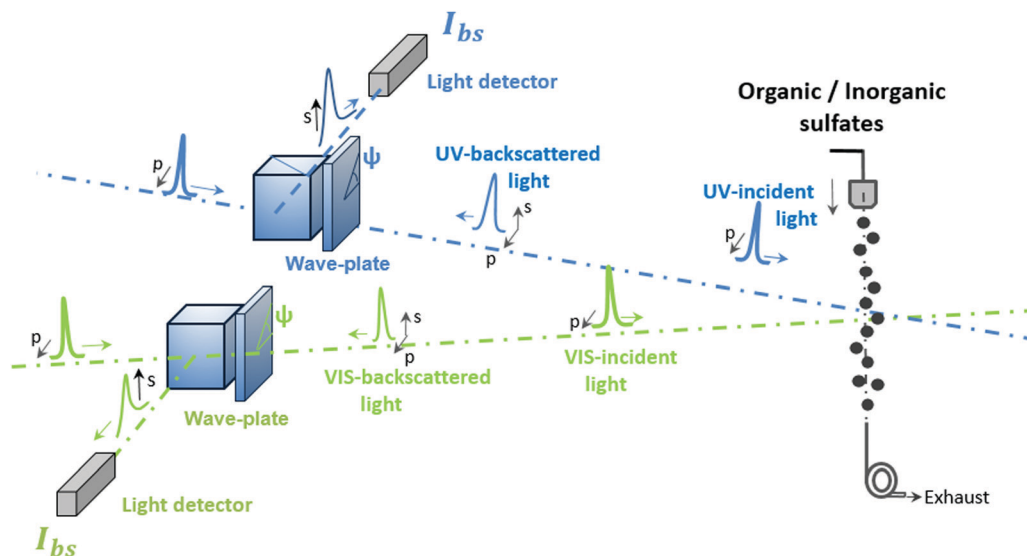


Fig. 2 Schematic of our laboratory (UV, VIS) laboratory polarimeter at exact backscattering angle of P_i ($180.0^\circ \pm 0.2^\circ$) for organic/inorganic sulfates embedded in ambient air. As extensively described in Miffre *et al.*,^{39,41,46} this laboratory experimental set-up, which relies on the robust scattering matrix formalism,⁴⁷ measures the detected backscattered intensity I_{bs} at two wavelengths (355, 532 nm) for different orientations ψ of a wave-plate.

atmospheric daytime conditions in isoprene-rich regions.²¹ The particle number was 10^6 particles per cubic centimeter. The maximum IEPOX gas-phase concentration was 409 ppb and the highest loading for sulfate particles was $2.8 \times 10^4 \mu\text{g m}^{-3}$. While the concentrations of IEPOX and aerosol seed particles were not atmospherically relevant, the use of these extreme experimental conditions were required to evaluate aerosol light backscattering using the steady-state-of-art instrumentation. After light backscattering, the generated aerosols were collected to quantify the concentration of IEPOX-SOA products by UHPLC/ESI-MS in negative ion mode. The optically-probed aerosols were

sampled at a flow rate of 5.2 L min^{-1} onto quartz filters (47 mm diameter – PALL). The detailed methodology used to extract filters has been described previously.⁴⁵ The sample extractions, the operating conditions, the standard preparation, and uncertainty estimates on IEPOX-OSS are described in detail in the ESI.[†]

Light backscattering experiments

Fig. 2 shows the schematic of the light backscattering experimental set-up. As extensively described by Miffre *et al.*,^{39,41} this laboratory experiment consists of a polarimeter operating in the exact backward scattering direction of P_i , defined with a high

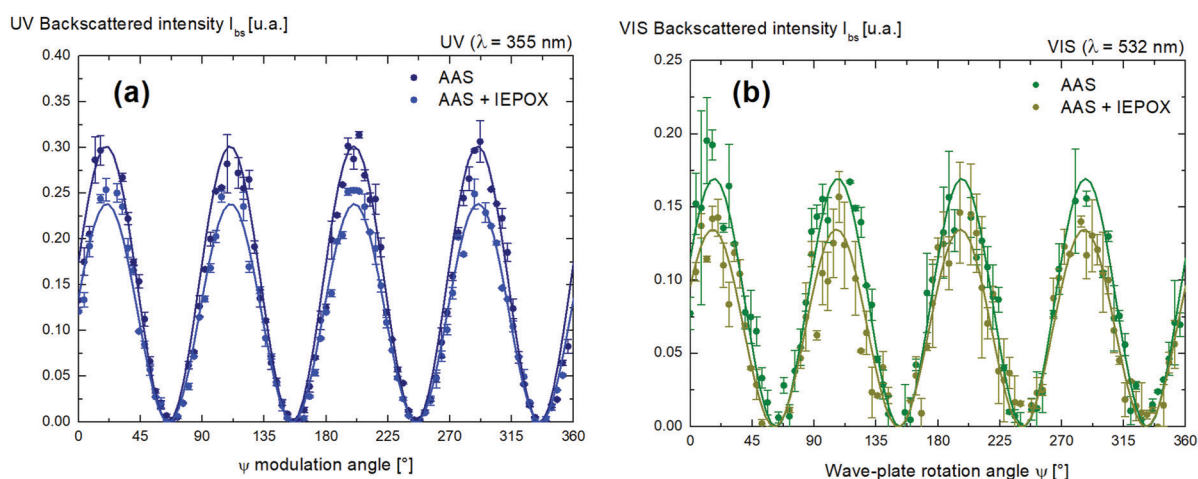


Fig. 3 Backscattered intensity acquisition curves: (a) detected light intensity I_{bs} backscattered by AAS (0 ppb IEPOX, dark blue), then AAS + IEPOX (409 ppb, blue) at 355 nm wavelength for different orientations ψ of a wave-plate, error bars are extensively described in a prior work.⁴¹ To reduce statistical error bars, each data point results from measurement repeated $N (= 5)$ times with corresponding mean and standard deviation. The variations of $I_{bs} = f(\psi)$ can be adjusted with a $\cos(4\psi)$ curve to precisely evaluate the maxima $I_{bs,M}$ of the detected backscattered intensity. These maxima, which corresponded to incident s-polarized radiation, provided precise evaluation of the backscattered intensity. (b) Same as (a) at wavelength 532 nm (AAS in dark green, AAS + IEPOX (409 ppb) in light green).

accuracy ($180.0^\circ \pm 0.2^\circ$), after precise alignment. The backscattered radiation from generated aerosols was discriminated from that due to ambient aerosols as this laboratory experiment is a time-of-flight experiment.^{39,41} As shown in Fig. 2 (see prior studies^{39,41} for more details), our laboratory experimental set-up consisted of two laboratory Pi-polarimeters, one for each wavelength (355 nm, 532 nm), operating simultaneously with negligible polarization and wavelength cross-talks.⁴¹ Following Fig. 2, each Pi-polarimeter was sensitive to the s-polarization component of the backscattered radiation and the corresponding detected intensity is then hereafter noted I_{bs} where (b,s)-subscripts refer to backscattering and to the detected s-polarization, respectively. Moreover, for spherical aerosols, which follow the Lorenz-Mie theory, the polarization state is preserved during the backscattering process. As a consequence, within our experimental set-up, the whole backscattered intensity can then be detected as I_{bs} when the incident electromagnetic radiation was s-polarized. Besides, when the incident radiation was p-polarized, the detected backscattered intensity I_{bs} canceled if particles were spherical, which provided a means to follow the particles deviation from isotropy.

Results and discussion

To gain in accuracy in the evaluation of the backscattered intensity, I_{bs} was recorded for different incident polarization states, obtained by rotating the ψ -angle of a quarter-wave plate, as displayed in Fig. 3 for inorganic sulfates (AAS particles) at UV and VIS-wavelengths (*i.e.*, 355 and 532 nm, respectively). Interestingly, the minima of $I_{bs} = f(\psi)$, which corresponded to an incident p-polarized radiation,⁴¹ were null, thus proving that inorganic sulfate aerosols remained spherical during the acquisition. As a consequence, the maxima $I_{bs,M}$ of $I_{bs} = f(\psi)$ corresponding to an incident s-polarized radiation⁴¹ can be used as a metric of the backscattered light intensity by AAS. A precise evaluation of these maxima was then performed by adjusting our experimental data points with a $\cos(4\psi)$ curve, as we previously demonstrated for mineral dust,⁴¹ by taking benefit from the robust scattering matrix formalism.⁴⁷ As a result, within our experimental set-up, the backscattered light intensity can be precisely evaluated from Fig. 3 as $I_{bs,M}$.

The $I_{bs,M}$ maxima were representative of a definite aerosol particle number density, chemical composition and size distribution.

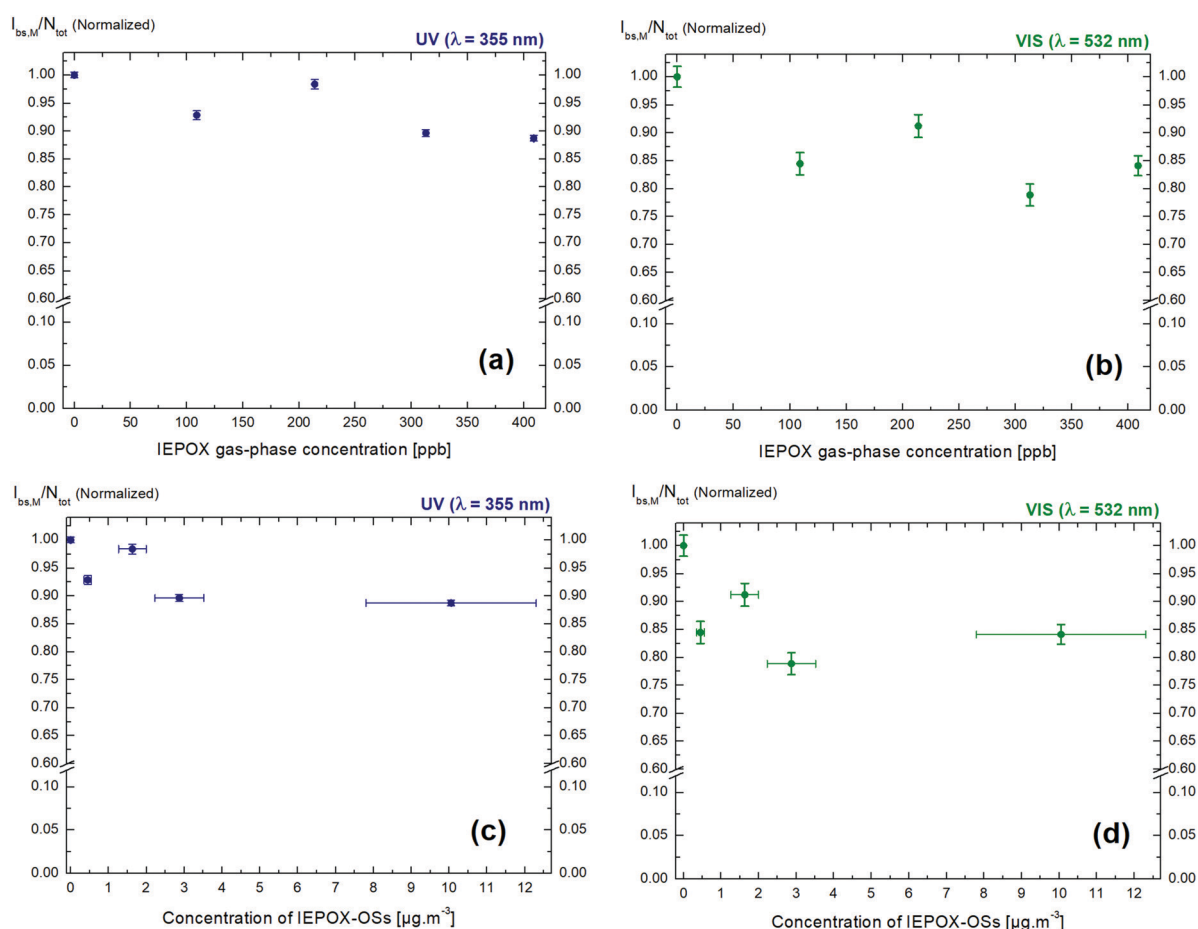


Fig. 4 (a and b) Upper figures: Normalized light backscattered intensity $I_{bs,M}/N_{tot}$ to account for potential variability in particle numbers and size distribution as a function of IEPOX gas-phase concentration [ppb] at wavelength 355 nm (a) then wavelength 532 nm (b). (c and d) Lower figures: Normalized light backscattered intensity $I_{bs,M}/N_{tot}$ as a function of IEPOX-OSs mass concentration. The AAS levels remained constant in the aerosol flow tube reactor. Increasing gas-phase IEPOX concentration corresponds to increasing IEPOX-OSs/inorganic sulfate ratio. Uncertainties ($\pm 22\%$, see S.I.) are reported for the concentrations of IEPOX-OSs.

Indeed, if the particle number or the size distribution had varied during the backscattering experiments, the maxima $I_{\text{bs},\text{M}}$ would not have remained constant when varying the wave-plates orientation. To quantify the modification of the backscattered light intensity I_{bs} through the reactive uptake of IEPOX on sulfate particles, the potential variation in particle number concentrations when considering IEPOX-SOA, instead of inorganic sulfates, was accounted for. For that, $I_{\text{bs},\text{M}}$ was normalized by the integral N_{Tot} of the particle number density over the generated particles size distribution, which is described in more detail in the ESI.† It should be noted that the uptake of IEPOX onto AAS did not change the electrical mobility size distribution of the particles; hence the decrease in backscattering is only due to changes in chemical composition. Measuring the light backscattered by organic-containing aerosol particles is a real experimental challenge due to the very low backscattering cross-section of such laboratory-generated aerosol particles with sizes in the hundreds of nanometers range only. However, the sensitivity achieved in the laboratory backscattering polarimeter was sufficiently high when the experimental conditions were pushed to high-level aerosol concentrations.

Fig. 4a and b show the decrease observed in the normalized backscattered light intensity $I_{\text{bs},\text{M}}/N_{\text{Tot}}$ when increasing the IEPOX gas phase concentration. Within our error bars, it is clear that reactive uptake of IEPOX induces a decrease in the light

backscattered by sulfate aerosol. This decrease is found to be slightly more pronounced in the visible spectral range (*i.e.*, –16% when exposed to gas-phase IEPOX concentrations of 409 ppb at 532 nm wavelength) than in the UV (*i.e.*, –12% at 355 nm wavelength). Such a spectral dependence may be due to several factors. One possible explanation is that organosulfates and/or oligomers (high-molecular weight compounds)^{16,17,48,49} absorb UV-light, which may modify the complex refractive index.⁴⁸ However, to be confirmed, this hypothesis would require authentic standards that cannot be synthesized at present, and it is hence beyond the scope of this contribution.

Fig. 4c and d present the normalized backscattered intensity $I_{\text{bs},\text{M}}/N_{\text{Tot}}$ as a function of the IEPOX-OS mass concentration in the aerosol phase. Within experimental uncertainties, the increase in the formation of organosulfates is correlated with a decrease in the backscattered light intensity, and this at both wavelengths. The decrease in the backscattered light intensity is observed even at low IEPOX-OS concentrations. The IEPOX-OS concentrations generated in the experiments correspond to a decrease in backscattering light intensity ranging from 2 to 12% at 355 nm wavelength, and from 9 to 21% at 532 nm wavelength, as depicted in Fig. 4. Though IEPOX-derived OSs represent a small subset of the total organic mass, the presence of such species, as well as other high-molecular weight compounds, can reduce aerosol light backscattering.

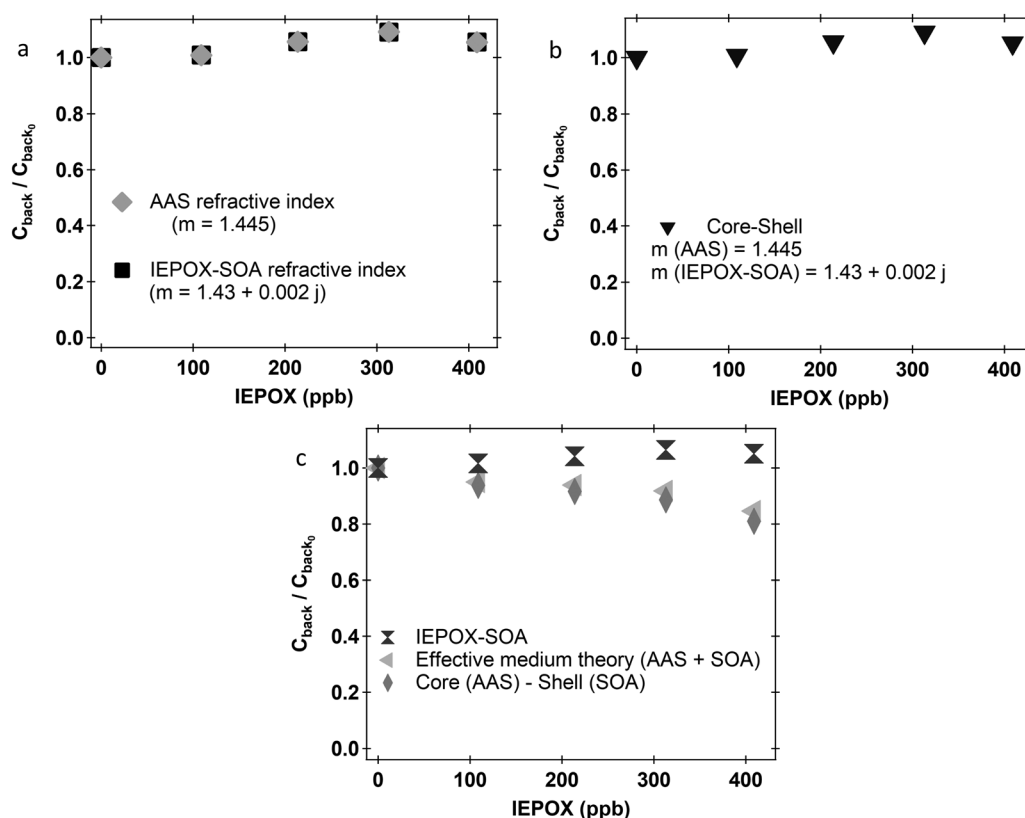


Fig. 5 Lorenz-Mie light scattering numerical simulation of the backscattering cross-section C_{back} normalized to $C_{\text{back},0}$ of inorganic particles at 532 nm wavelength, considering the SD given in the S.M. for (a) AAS and IEPOX-derived SOA refractive index, (b) a core-shell model using the above refractive indices and volume fractions, (c) a core-shell model, considering $1.43 + 0.5j$ for the IEPOX-derived SOA complex refractive index, together with $C_{\text{back}}/C_{\text{back},0}$ for that refractive index and from effective medium theory.

To interpret the observed decrease in light backscattering, light scattering numerical simulations have been performed by applying the Lorenz–Mie theory to compute the backscattering cross-section C_{back} (resp. $C_{\text{back},0}$) of organic (resp. inorganic) particles. Indeed, our laboratory polarimeter showed that the shape of these aerosols remained spherical during the experiments as the minima of $I_{\text{bs},M}$ were null. Then, and as discussed in the introduction, the backscattering process only depends on the aerosol particle number concentration, size distribution (SD) and chemical composition, through the particles complex refractive index. The backscattering cross-sections C_{back} were then computed using the particles SD presented in the ESI† for the mixture of AAS with IEPOX. As shown in the ESI†, special care has been taken in our experiments to ensure the SD to be constant during all the acquisitions. As a first step, C_{back} was computed for the refractive index of AAS ($m = 1.445$)⁵⁰ and IEPOX-derived SOA ($m = 1.43 + 0.002j$),⁵¹ Fig. 5, respectively. Hence, the observed decrease in the backscattering cross-section C_{back} cannot be explained by size effects alone and was therefore related to optical index effects also, as the solutions evolve (Fig. 5).

To account for the presence of both AAS and IEPOX-derived SOA compounds, we applied effective medium theories, by applying the Aspens formula,⁴⁷ providing the effective particles complex refractive index of a backscattering medium containing a mixture of AAS and IEPOX-derived SOA products. As displayed in Fig. 5b however, the variations of $C_{\text{back}}/C_{\text{back},0}$ did not more faithfully reproduce our laboratory observations when considering AAS volume fractions in the AAS and IEPOX-derived SOA particle mixtures ranging from 0.96 to 1.00, with 0.02 step, which is consistent with the results from our chemical analyses of the aerosol filter samples. As a result, we investigated the effect on C_{back} of a possible change in the internal structure of the particles. Indeed, the reactive uptake of IEPOX is known to produce core–shell structures.^{11,21,22} To investigate the case of a stratified dielectric sphere (*i.e.*, a spherical inorganic core coated by a spherical organic shell), we applied the numerical code from Toon and Ackermann,⁵² which is an extension of the Lorenz–Mie theory, suitable for thin film absorbent particles as it was expected in our experiments. When adjusting the core/shell radius to consider the above volume fractions, we reproduced a part of the observed decrease in C_{back} , as depicted in Fig. 5c. Fig. 5c shows that considering an IEPOX refractive index of $1.43 + 0.5j$ leads to a decrease in the backscattering cross-section $C_{\text{back}}/C_{\text{back},0}$ by about 18% at 409 ppb at 532 nm wavelength. This trend lies in the same range as the measured decrease in light backscattering that reaches 16% for visible light backscattering (*i.e.* at 532 nm wavelength and 409 ppb of IEPOX). Nevertheless, this decrease in the visible light backscattering can also be due to the absorption of high molecular weight compounds as above stated. A plausible explanation is that the considered refractive index for IEPOX-derived SOA products reported in the literature did not represent our laboratory experimental conditions, where other values for both the real and imaginary parts of the refraction index were required. To be confirmed, more laboratory and numerical intensive work on the IEPOX complex refractive index are required to accurately determine the complex refractive index of IEPOX-derived SOA particles, which is beyond the scope of this contribution.

Conclusions

In this paper, in a context where isoprene epoxydiols are the most important isoprene SOA precursors, we present an unexpected trend in the backscattering coefficient of SOA containing sulfate and organic material: in both the UV and VIS spectral ranges, sulfate aerosol light backscattering is decreased by reactive uptake of IEPOX on acidified inorganic sulfate aerosol particles. This laboratory finding has been obtained by taking advantage of an accurate and extremely sensitive polarimeter operating at the exact backward scattering angle of π as the laboratory-generated particles, whose size lies in the hundreds of nanometer range, exhibited a very low backscattering cross-section. When acidified sulfate particles ($2.8 \times 10^4 \mu\text{g m}^{-3}$) were exposed to the largest IEPOX concentration (*i.e.*, 409 ppb), the observed decrease reaches 12% at 355 nm wavelength and 16% at 532 nm wavelength. Possible explanations for the observed decrease in light backscattering were investigated using existing literature and Lorenz–Mie light scattering numerical simulations of the particle backscattering cross-section of organic/inorganic particles. We showed that the observed decrease can only be explained by considering effects from the complex optical refractive index. Notably, we discussed that the formation of an inorganic core–organic shell structure can be key for explaining the reported decrease, though effective medium theories may also be key. The formation of a high-absorbing organic coating, corresponding to a large imaginary part of the optical refractive index of IEPOX-SOA of about 0.5, was necessary to explain our experimental results. These results should be improved in laboratory experiments by considering more complex particle chemistry or micro-physical structure. In summary, acid-driven particle-phase and/or heterogeneous chemistry has the potential to change the optical properties of aerosols through both chemical and physical pathways, opening routes for future research. Indeed, the development of such a precise optical system will allow for quantification of the radiative effects of aerosol particles impacted by atmospheric ageing.

Author contributions

C. Dubois: formal analysis, vi-sualization, writing – original draft, D. Cholleton: methodology, software, formal analysis, investigation vi-sualization, writing – review & editing, R. Gemayel: vi-sualization, Y. Chen: vi-sualization, J. D. Surratt: formal analysis, investigation, vi-sualization, resources, project administration, funding acquisition, C. George: methodology, formal analysis investigation, validation, project administration, funding acquisition, P. Rairoux: methodology, formal analysis, investigation validation, project administration, funding acquisition, A. Miffre: methodology, formal analysis investigation, software, vi-sualization, writing – original draft, writing – review & editing validation, project administration, funding acquisition, M. Riva: methodology, formal analysis, investigation vi-sualization, writing – review & editing, project administration, funding acquisition.

Conflicts of interest

There are no conflicts to declare.

Acknowledgements

Support for C. D. by the Chemistry doctoral school at the University of Lyon is acknowledged. We thank Avram Gold and Zhenfa Zhang at the University of North Carolina at Chapel Hill for providing the authentic standards of IEPOX and IEPOX-OSs (*i.e.*, 2-methyltetrol sulfate). J. D. S. and Y. C. acknowledge support from the United States National Science Foundation (NSF) under Atmospheric and Geospace (AGS) Grant 1703535. We thank Sophie Tomaz for useful discussions. The light backscattering experiment was funded by the CNRS Institute of Physics and Lyon University.

References

- Climate change 2013: the physical science basis; summary for policymakers, a report of Working Group I of the IPCC, technical summary, a report accepted by Working Group I of the IPCC but not approved in detail and frequently asked questions; part of the Working Group I contribution to the fifth assessment report of the Intergovernmental Panel on Climate Change, ed. T. F. Stocker and Intergovernmental Panel on Climate Change, Intergovernmental Panel on Climate Change, New York, 2013.
- R. J. Charlson, J. Langner, H. Rodhe, C. B. Leovy and S. G. Warren, Perturbation of the northern hemisphere radiative balance by backscattering from anthropogenic sulfate aerosols, *Tellus A*, 1991, **43**, 152–163.
- K. E. Taylor and J. E. Penner, Response of the climate system to atmospheric aerosols and greenhouse gases, *Nature*, 1994, **369**, 734–737.
- J. Feichter, U. Lohmann and I. Schult, The atmospheric sulfur cycle in ECHAM-4 and its impact on the shortwave radiation, *Clim. Dyn.*, 1997, **13**, 235–246.
- D. Goto, T. Nakajima, T. Takemura and K. Sudo, A study of uncertainties in the sulfate distribution and its radiative forcing associated with sulfur chemistry in a global aerosol model, *Atmos. Chem. Phys.*, 2011, **11**(21), 10889–10910.
- O. Boucher, D. Randall, P. Artaxo, C. Bretherton, G. Feingold, P. Forster, V.-M. Kerminen, Y. Kondo, H. Lia, U. Lohmann, P. Rasch, S. K. Satheesh, S. Sherwood, B. Stevens and X. Y. Zhang, Clouds and Aerosols, in *Climate Change 2013: The Physical Science Basis. Contribution of Working Group I to the Fifth Assessment Report of the Intergovernmental Panel on Climate Change*, ed. T. F. Stocker, D. Qin, G.-K. Plattner, M. Tignor, S. K. Allen, J. Boschung, A. Nauels, Y. Xia, V. Bex and P. M. Midgley, Cambridge University Press, Cambridge, United Kingdom and New York, NY, USA, 2013.
- J. Haywood and O. Boucher, Estimates of the direct and indirect radiative forcing due to tropospheric aerosols: A review, *Rev. Geophys.*, 2000, **38**, 513–543.
- J. Zhu, J. E. Penner, F. Yu, S. Sillman, M. O. Andreae and H. Coe, Decrease in radiative forcing by organic aerosol nucleation, climate, and land use change, *Nat. Commun.*, 2019, **10**, 423.
- J. K. Kodros, C. E. Scott, S. C. Farina, Y. H. Lee, C. L'Orange, J. Volckens and J. R. Pierce, Uncertainties in global aerosols and climate effects due to biofuel emissions, *Atmos. Chem. Phys.*, 2015, **15**, 8577–8596.
- C. E. Scott, D. V. Spracklen, J. R. Pierce, I. Riipinen, S. D. D'Andrea, A. Rap, K. S. Carslaw, P. M. Forster, P. Artaxo, M. Kulmala, L. V. Rizzo, E. Swietlicki, G. W. Mann and K. J. Pringle, Impact of gas-to-particle partitioning approaches on the simulated radiative effects of biogenic secondary organic aerosol, *Atmos. Chem. Phys.*, 2015, **15**, 12989–13001.
- M. Riva, Y. Chen, Y. Zhang, Z. Lei, N. Olson, H. C. Boyer, S. Narayan, L. D. Yee, H. Green, T. Cui, Z. Zhang, K. D. Baumann, M. Fort, E. S. Edgerton, S. Budisulistiorini, C. A. Rose, I. Ribeiro, R. L. e Oliveira, E. Santos, S. Szopa, C. Machado, Y. Zhao, E. Alves, S. de Sa, W. Hu, E. Knipping, S. Shaw, S. Duvoisin Junior, R. A. F. de Souza, B. B. Palm, J. L. Jimenez, M. Glasius, A. H. Goldstein, H. O. T. Pye, A. Gold, B. J. Turpin, W. Vizuete, S. T. Martin, J. Thornton, C. S. Dutcher, A. P. Ault and J. D. Surratt, Increasing Isoprene Epoxidiol-to-Inorganic Sulfate Aerosol (IEPOX:Sulf_{inorg}) Ratio Results in Extensive Conversion of Inorganic Sulfate to Organosulfur Forms: Implications for Aerosol Physicochemical Properties, *Environ. Sci. Technol.*, 2019, **53**(15), 8682–8694.
- K. M. Shakya and R. E. Peltier, Investigating Missing Sources of Sulfur at Fairbanks, Alaska, *Environ. Sci. Technol.*, 2013, **47**, 9332–9338.
- K. M. Shakya and R. E. Peltier, Non-sulfate sulfur in fine aerosols across the United States: Insight for organosulfate prevalence, *Atmos. Environ.*, 2015, **100**, 159–166.
- M. P. Tolocka and B. Turpin, Contribution of Organosulfur Compounds to Organic Aerosol Mass, *Environ. Sci. Technol.*, 2012, **46**, 7978–7983.
- J. D. Surratt, Y. Gómez-González, A. W. H. Chan, R. Vermeulen, M. Shahgholi, T. E. Kleindienst, E. O. Edney, J. H. Offenberg, M. Lewandowski, M. Jaoui, W. Maenhaut, M. Claeys, R. C. Flagan and J. H. Seinfeld, Organosulfate Formation in Biogenic Secondary Organic Aerosol, *J. Phys. Chem. A*, 2008, **112**, 8345–8378.
- J. D. Surratt, A. W. H. Chan, N. C. Eddingsaas, M. Chan, C. L. Loza, A. J. Kwan, S. P. Hersey, R. C. Flagan, P. O. Wennberg and J. H. Seinfeld, Reactive intermediates revealed in secondary organic aerosol formation from isoprene, *Proc. Natl. Acad. Sci. U. S. A.*, 2010, **107**, 6640–6645.
- Y.-H. Lin, Z. Zhang, K. S. Docherty, H. Zhang, S. H. Budisulistiorini, C. L. Rubitschun, S. L. Shaw, E. M. Knipping, E. S. Edgerton, T. E. Kleindienst, A. Gold and J. D. Surratt, Isoprene Epoxidiols as Precursors to Secondary Organic Aerosol Formation: Acid-Catalyzed Reactive Uptake Studies with Authentic Compounds, *Environ. Sci. Technol.*, 2012, **46**, 250–258.
- C. J. Gaston, T. P. Riedel, Z. Zhang, A. Gold, J. D. Surratt and J. A. Thornton, Reactive Uptake of an Isoprene-Derived

- Epoxydiol to Submicron Aerosol Particles, *Environ. Sci. Technol.*, 2014, **48**, 11178–11186.
- 19 T. P. Riedel, Y.-H. Lin, S. H. Budisulistiorini, C. J. Gaston, J. A. Thornton, Z. Zhang, W. Vizuete, A. Gold and J. D. Surratt, Heterogeneous Reactions of Isoprene-Derived Epoxides: Reaction Probabilities and Molar Secondary Organic Aerosol Yield Estimates, *Environ. Sci. Technol. Lett.*, 2015, **2**, 38–42.
 - 20 M. Riva, D. M. Bell, A.-M. K. Hansen, G. T. Drozd, Z. Zhang, A. Gold, D. Imre, J. D. Surratt, M. Glasius and A. Zelenyuk, Effect of Organic Coatings, Humidity and Aerosol Acidity on Multiphase Chemistry of Isoprene Epoxydiols, *Environ. Sci. Technol.*, 2016, **50**, 5580–5588.
 - 21 Y. Zhang, Y. Chen, A. T. Lambe, N. E. Olson, Z. Lei, R. L. Craig, Z. Zhang, A. Gold, T. B. Onasch, J. T. Jayne, D. R. Worsnop, C. J. Gaston, J. A. Thornton, W. Vizuete, A. P. Ault and J. D. Surratt, Effect of the Aerosol-Phase State on Secondary Organic Aerosol Formation from the Reactive Uptake of Isoprene-Derived Epoxydiols (IEPOX), *Environ. Sci. Technol. Lett.*, 2018, **5**, 167–174.
 - 22 N. Olson, Z. Lei, R. L. Craig, Y. Zhang, Y. Chen, A. T. Lambe, Z. Zhang, A. Gold, J. D. Surratt and A. P. Ault, Reactive Uptake of Isoprene Epoxydiols Increases the Viscosity of the Core of Phase-Separated Aerosol Particles, *ACS Earth Space Chem.*, 2019, **3**(8), 1402–1414.
 - 23 F. Paulot, J. D. Crounse, H. G. Kjaergaard, A. Kurten, J. M. St. Clair, J. H. Seinfeld and P. O. Wennberg, Unexpected Epoxide Formation in the Gas-Phase Photooxidation of Isoprene, *Science*, 2009, **325**, 730–733.
 - 24 A. B. Guenther, X. Jiang, C. L. Heald, T. Sakulyanontvittaya, T. Duhl, L. K. Emmons and X. Wang, The Model of Emissions of Gases and Aerosols from Nature version 2.1 (MEGAN2.1): an extended and updated framework for modeling biogenic emissions, *Geosci. Model Dev.*, 2012, **5**, 1471–1492.
 - 25 W. Wang, I. Kourtchev, B. Graham, J. Cafmeyer, W. Maenhaut and M. Claeys, Characterization of oxygenated derivatives of isoprene related to 2-methyltetrols in Amazonian aerosols using trimethylsilylation and gas chromatography/ion trap mass spectrometry, *Rapid Commun. Mass Spectrom.*, 2005, **19**, 1343–1351.
 - 26 M. Claeys, Formation of Secondary Organic Aerosols Through Photooxidation of Isoprene, *Science*, 2004, **303**, 1173–1176.
 - 27 M. Claeys, W. Wang, A. C. Ion, I. Kourtchev, A. Gelencsér and W. Maenhaut, Formation of secondary organic aerosols from isoprene and its gas-phase oxidation products through reaction with hydrogen peroxide, *Atmos. Environ.*, 2004, **38**, 4093–4098.
 - 28 J. D. Surratt, S. M. Murphy, J. H. Kroll, N. L. Ng, L. Hildebrandt, A. Sorooshian, R. Szmigielski, R. Vermeylen, W. Maenhaut, M. Claeys, R. C. Flagan and J. H. Seinfeld, Chemical Composition of Secondary Organic Aerosol Formed from the Photooxidation of Isoprene, *J. Phys. Chem. A*, 2006, **110**, 9665–9690.
 - 29 J. D. Surratt, J. H. Kroll, T. E. Kleindienst, E. O. Edney, M. Claeys, A. Sorooshian, N. L. Ng, J. H. Offenberg, M. Lewandowski, M. Jaoui, R. C. Flagan and J. H. Seinfeld, Evidence for Organosulfates in Secondary Organic Aerosol, *Environ. Sci. Technol.*, 2007, **41**, 517–527.
 - 30 M. Glasius, M. S. Bering, L. D. Yee, S. S. de Sá, G. Isaacman-VanWertz, R. A. Wernis, H. M. J. Barbosa, M. L. Alexander, B. B. Palm, W. Hu, P. Campuzano-Jost, D. A. Day, J. L. Jimenez, M. Shrivastava, S. T. Martin and A. H. Goldstein, Organosulfates in aerosols downwind of an urban region in central Amazon, *Environ. Sci.: Processes Impacts*, 2018, **20**, 1546–1558.
 - 31 Y. Gómez-González, J. D. Surratt, F. Cuyckens, R. Szmigielski, R. Vermeylen, M. Jaoui, M. Lewandowski, J. H. Offenberg, T. E. Kleindienst, E. O. Edney, F. Blockhuys, C. Van Alsenoy, W. Maenhaut and M. Claeys, Characterization of organosulfates from the photooxidation of isoprene and unsaturated fatty acids in ambient aerosol using liquid chromatography/(-) electrospray ionization mass spectrometry, *J. Mass Spectrom.*, 2008, **43**, 371–382.
 - 32 A. P. S. Hettiyadura, I. M. Al-Naiema, D. D. Hughes, T. Fang and E. A. Stone, Organosulfates in Atlanta, Georgia: anthropogenic influences on biogenic secondary organic aerosol formation, *Atmos. Chem. Phys.*, 2019, **19**, 3191–3206.
 - 33 Y. Zhang, Y. Chen, Z. Lei, N. E. Olson, M. Riva, A. R. Koss, Z. Zhang, A. Gold, J. T. Jayne, D. R. Worsnop, T. B. Onasch, J. H. Kroll, B. J. Turpin, A. P. Ault and J. D. Surratt, Joint Impacts of Acidity and Viscosity on the Formation of Secondary Organic Aerosol from Isoprene Epoxydiols (IEPOX) in Phase Separated Particles, *ACS Earth Space Chem.*, 2019, **3**, 2646–2658.
 - 34 G. David, B. Thomas, T. Nousiainen, A. Miffre and P. Rairoux, Retrieving simulated volcanic, desert dust and sea-salt particle properties from two/three-component particle mixtures using UV-VIS polarization lidar and T matrix, *Atmos. Chem. Phys.*, 2013, **13**, 6757–6776.
 - 35 H. Van de Hulst, *Light Scattering by Small Particle*, John Wiley & Sons, Inc., New York, 1957, pp. 114–130.
 - 36 T. Mehri, O. Kemppinen, G. David, H. Lindqvist, J. Tyynelä, T. Nousiainen, P. Rairoux and A. Miffre, Investigating the size, shape and surface roughness dependence of polarization lidars with light-scattering computations on real mineral dust particles: Application to dust particles' external mixtures and dust mass concentration retrievals, *Atmos. Res.*, 2018, **203**, 44–61.
 - 37 M. I. Mishchenko, Electromagnetic scattering by nonspherical particles: A tutorial review, *J. Quant. Spectrosc. Radiat. Transfer*, 2009, **110**, 808–832.
 - 38 A. Haddrell, G. Rovelli, D. Lewis, T. Church and J. Reid, Identifying time-dependent changes in the morphology of an individual aerosol particle from its light scattering pattern, *Aerosol Sci. Technol.*, 2019, **53**, 1334–1351.
 - 39 A. Miffre, D. Cholleton and P. Rairoux, Laboratory evaluation of the scattering matrix elements of mineral dust particles from 176.0° up to 180.0°-exact backscattering angle, *J. Quant. Spectrosc. Radiat. Transfer*, 2019, **222–223**, 45–59.
 - 40 M. I. Mishchenko, Maxwell's equations, radiative transfer, and coherent backscattering: A general perspective, *J. Quant. Spectrosc. Radiat. Transfer*, 2006, **101**, 540–555.

- 41 A. Miffre, T. Mehri, M. Francis and P. Rairoux, UV-VIS depolarization from Arizona Test Dust particles at exact backscattering angle, *J. Quant. Spectrosc. Radiat. Transfer*, 2016, **169**, 79–90.
- 42 C. J. Gaston, T. P. Riedel, Z. Zhang, A. Gold, J. D. Surratt and J. A. Thornton, Reactive Uptake of an Isoprene-Derived Epoxydiol to Submicron Aerosol Particles, *Environ. Sci. Technol.*, 2014, **48**, 11178–11186.
- 43 E. L. D'Ambro, S. Schobesberger, C. J. Gaston, F. D. Lopez-Hilfiker, B. H. Lee, J. Liu, A. Zelenyuk, D. Bell, C. D. Cappa, T. Helgestad, Z. Li, A. Guenther, J. Wang, M. Wise, R. Caylor, J. D. Surratt, T. Riedel, N. Hyttinen, V.-T. Salo, G. Hasan, T. Kurtén, J. E. Shilling and J. A. Thornton, Chamber-based insights into the factors controlling epoxydiol (IEPOX) secondary organic aerosol (SOA) yield, composition, and volatility, *Atmos. Chem. Phys.*, 2019, **19**, 11253–11265.
- 44 Z. Zhang, Y.-H. Lin, H. Zhang, J. D. Surratt, L. M. Ball and A. Gold, Technical Note: Synthesis of isoprene atmospheric oxidation products: isomeric epoxydiols and the rearrangement products *cis*- and *trans*-3-methyl-3,4-dihydroxytetrahydrofuran, *Atmos. Chem. Phys.*, 2012, **12**, 8529–8535.
- 45 X. Wang, N. Hayeck, M. Brüggemann, L. Yao, H. Chen, C. Zhang, C. Emmelin, J. Chen, C. George and L. Wang, Chemical Characteristics of Organic Aerosols in Shanghai: A Study by Ultrahigh-Performance Liquid Chromatography Coupled With Orbitrap Mass Spectrometry: Organic Aerosols in Shanghai, *J. Geophys. Res.: Atmos.*, 2017, **122**, 11703–11722.
- 46 L. Paulien, R. Ceolato, F. Foissard, P. Rairoux and A. Miffre, (UV, VIS) laboratory evaluation of the lidar depolarization ratio of freshly emitted soot aggregates from pool fire in ambient air at exact backscattering angle, *J. Quant. Spectrosc. Radiat. Transfer*, 2021, **260**, 107451.
- 47 M. I. Mishchenko, L. D. Travis and A. A. Lacis, *Scattering, absorption, and emission of light by small particles*, Cambridge University Press, Cambridge; New York, 2002.
- 48 Y.-H. Lin, S. H. Budisulistiorini, K. Chu, R. A. Siejack, H. Zhang, M. Riva, Z. Zhang, A. Gold, K. E. Kautzman and J. D. Surratt, Light-Absorbing Oligomer Formation in Secondary Organic Aerosol from Reactive Uptake of Isoprene Epoxydiols, *Environ. Sci. Technol.*, 2014, **48**, 12012–12021.
- 49 M. Riva, S. H. Budisulistiorini, Z. Zhang, A. Gold, J. A. Thornton, B. J. Turpin and J. D. Surratt, Multiphase reactivity of gaseous hydroperoxide oligomers produced from isoprene ozonolysis in the presence of acidified aerosols, *Atmos. Environ.*, 2017, **152**, 314–322.
- 50 M. I. Cotterell, R. E. Willoughby, B. R. Bzdek, A. J. Orr-Ewing and J. P. Reid, A complete parameterisation of the relative humidity and wavelength dependence of the refractive index of hygroscopic inorganic aerosol particles, *Atmos. Chem. Phys.*, 2017, **17**, 9837–9851.
- 51 T. Nakayama, K. Sato, T. Imamura and Y. Matsumi, Effect of Oxidation Process on Complex Refractive Index of Secondary Organic Aerosol Generated from Isoprene, *Environ. Sci. Technol.*, 2018, **52**, 2566–2574.
- 52 T. P. Ackerman and O. B. Toon, Absorption of visible radiation in atmosphere containing mixtures of absorbing and nonabsorbing particles, *Appl. Opt.*, 1981, **20**, 3661.